MODELING OF INTERNAL INJECTION AND BEAM DYNAMICS FOR HIGH POWER RF ACCELERATOR *

M.A. Tiunov#, V.L. Auslender, M.M. Karliner, G.I. Kuznetsov, I.G. Makarov,
A.D. Panfilov, V.V. Tarnetsky, Budker INP, 630090 Novosibirsk, Russia

Abstract

A new high power electron accelerator for industrial applications is developed in Novosibirsk. Main parameters of the accelerator are: operating frequency of 177 MHz, energy of electrons of 5 MeV, average beam power up to 300 kW. The accelerator consists of a chain of accelerating cavities, connected by the on-axis coupling cavities with coupling slots in the walls. A triode RF gun on the base of cathode-grid assembly placed on the wall of the first accelerating cell is used for internal injection of electrons. The paper presents the results of modelling and optimization of the accelerating structure, internal injection, and beam dynamics.

INTRODUCTION

High power RF accelerator prototype for industrial applications is developed now in BINP, Novosibirsk [1]. Main parameters of the accelerator are: operating frequency of 177 MHz, energy of electrons of 5 MeV, average beam power up to 300 kW at duty factor of 14% [1,2]. General view of the accelerator is shown on Fig. 1.

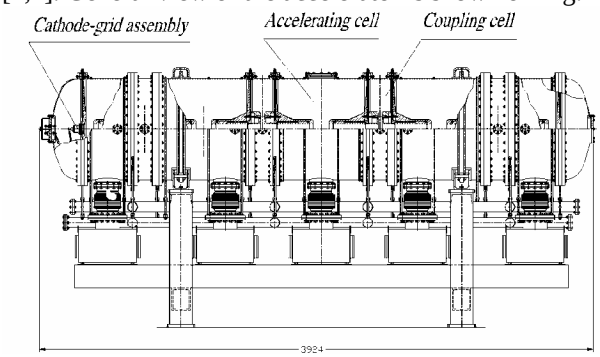

Figure 1: General view of accelerator.

The electrons are accelerated in the multi-resonator standing wave structure with on-axis coupling resonators. Such design makes it possible to decrease power losses in each resonator comparing to the single-resonator accelerator (at the same average beam power level) and to obtain the electron efficiency of the accelerator of about 70%.

The internal beam injection from the cathode-grid assembly, which is placed directly to the first accelerating gap, will be used. This concept permits us to sufficiently simplify the design and reduce the cost of the accelerator respectively, as well as to improve its reliability and reduce the maintenance charges.

Two important tasks may be emphasized from a quantity of problems that must be solved for accelerator prototype successful development:

- achievement of the required value of the pulse beam current at relatively low electric field strength in the accelerating gaps comparing with the single-resonator accelerator;
- lossless transportation of a powerful electron beam through the accelerating structure without usage of electro- and magnetostatic lenses.

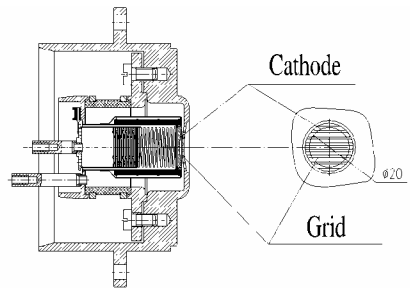

Figure 2: General view of cathode-grid assembly.

To solve these problems, a new cathode-grid assembly was designed. General view of this important component is shown on Fig. 2.

The report describes results of detailed simulation of internal injection and beam dynamics in ILU-12 accelerator. Computer simulations were performed in long-wave approximation using SAM [3] and ExtraSAM [4] codes, modified for solution of the problems mentioned above.

INTERNAL INJECTION SIMULATION

2D Model of the Cathode-Grid Assembly Cell

Figure 3 presents the cathode-grid assembly model for 2D simulation. The main geometric parameters of the assembly are: the cathode-grid gap *d*, step of the grid *h*, and diameter of wires *D*.

The computer optimization of these parameters was carried out with ExtraSAM program package [4] modified for time-dependent modeling of the effect of emission limitation by the beam space charge. All the cathode-grid assembly simulation results presented below were obtained using the following optimized geometric parameters: d = 1.5 mm, h = 3 mm, D = 1 mm.

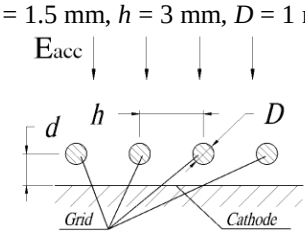

Figure 3: 2D model of the cathode-grid assembly.

*Work supported by DOE, ISTC Project #2550
#tiunov@inp.nsk.su

Figure 4 shows the simulation results for a single cell of the cathode-grid assembly at the amplitude of the accelerating field at the grid plane of 85 kV/cm.

The control cathode-grid voltage has the following time dependence:

$$Ug(t) = U_0 + U_1 \cdot \sin(\omega t + \varphi_1), \qquad (1)$$

here $U_0 = -2.1 kV$ is the constant bias voltage on the cathode-grid assembly, $U_1 = 2 kV$ and $\varphi_1 = 60°$ are amplitude and phase shift of the additional bias RF voltage at operating frequency, $\omega t = 2\pi f t$ – phase of the accelerating field. The simulations were performed for the accelerating field phase range from 0˚ to 140˚ at maximal number of phase layers of particles *Nφ*=140.

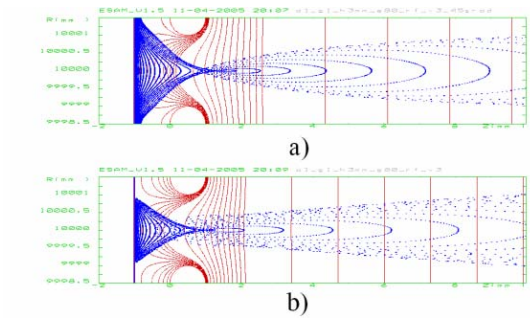

Figure 4: Results of time-dependent modeling of single cell of the cathode-grid assembly: a) maximum cathode current at the accelerating field phase of 45º; b) half of maximum cathode current at phase of 70º (lines – equipotential lines, points – phase layers of particles).

3D Model of the Cathode-Grid Assembly

A simulation 3D model of the cathode-grid assembly (see Fig. 5) was developed to describe the beam injection into the accelerator. It considers existence of seven various-length longitudinal slots in the grid located in front of the 20 mm cathode. Besides, the spherical form of the grid and cathode is also taken into account.

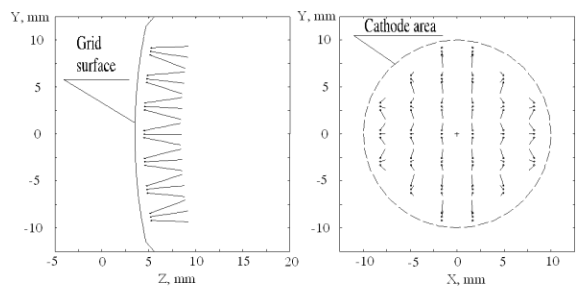

Figure 5: 3D model of the cathode-grid assembly for *Nx*=6 and *Ny*=3: a) YZ projection; b) XY projection.

The beam time-dependent flow characteristics from a single cathode-grid assembly cell at 1 mm distance from the grid surface were used for calculation of the macroparticles starting parameters in 3D beam dynamics simulation. Here, the cathode start transverse coordinates for each slot was defined equidistantly, a total of *Ny* points.

To describe the beam parameters along slots, the slots were divided into equal microcells, at that their maximal number *Nx* was defined for the central slot. Length of each cell was determined by condition that the microcell central point did not leave the cathode area.

BEAM DYNAMICS SIMULATION

Calculation of Current Micropulse and Beam Spectrum

Calculation of the macroparticle dynamics in the accelerator starts at a distance of 1 mm behind the grid. Here, the transit effect leads to delay in electron departure from the cathode-grid assembly and deformation of the current micropulse form.

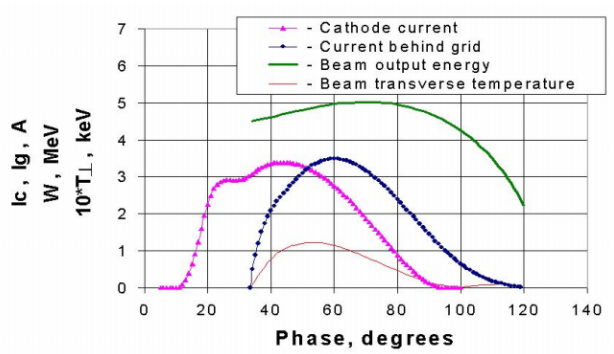

Figure 6: Accelerating field on the cathode phase dependencies of the current micropulse and beam output parameters.

So, by time-dependent code together with calculation of current micropulse form at the cathode, the calculation of the current micropulse form behind the grid was carried out. On Figure 6 the curves with triangles and circles show the simulation results for current micropulse form on the cathode and at a distance of 1 mm behind the grid respectively.

3D beam dynamics simulation in the accelerator was carried out by modified SAM code with taking into account the current micropulse form behind the grid. Simulation results for the accelerating field phase dependencies of the beam energy and effective transverse temperature at the accelerator output are also presented in Fig. 6.

As may be seen from Fig. 6, the electron output energy substantially depends on the accelerating field phase on the cathode. Just this fact leads to necessity of the use of an additional first harmonic voltage at the cathode-grid gap to shift the current micropulse into the acceptable phase area and narrowing the beam energy spectrum. As a result, a mean square electron energy deviation from the beam average energy 4.83 MeV amounts to only 3.3 %.

Beneficial effect of an additional first harmonic using was experimentally proven at the present single-gap accelerator ILU-10 [1].

Beam Transportation Through the Accelerator

The calculated average output power of the beam with parameters presented in Fig. 6 is equal to 305 kW at duty factor of 14%. For such high-power beam the problem of lossless transportation becomes very important. Here, it is necessary to keep in mind the space charge influence on the electron transverse dynamics, especially at the first acceleration stage. So, for every macroparticle the effective beam space charge transverse field was calculated:

$$E_r^{(q)} = \frac{Z_0 \cdot J(t) \cdot r_0^2}{2 \cdot \pi \cdot r \cdot \beta \cdot \gamma^2}, \qquad (2)$$

here $Z_0 \approx 120 \cdot \pi (\Omega)$ is the impedance of free space, $J(t)$ is the dynamic value of the average emission current density for a macroparticle with starting time t, calculated by time-dependent code; r_0 is the macro particle starting radius; r, β and γ are the current values of macroparticle radius, relative velocity and relativistic factor.

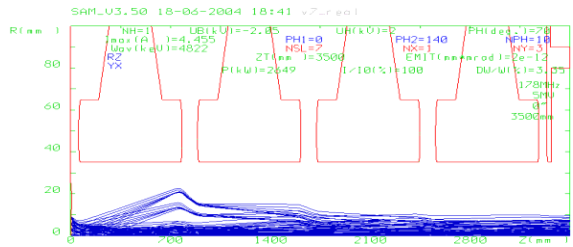

Figure 7: Typical view of electron trajectories in the accelerator.

Figure 7 presents a typical view of electron trajectories in the accelerator (*Nx*=1, *Ny*=3, *Nφ*=10). As is obvious from the figure, the beam consists of the central core formed by electrons started from centers of slots in the grid and moved transversely to the cathode. Also there is a noticeable halo formed by electrons started from edges of slots and moved at some angle to the normal. The results presented were obtained after optimization of the cathode-grid assembly sphere radius of curvature and accelerator aperture. Simulations proved the possibility to transport the beam through the accelerator at the expense of aperture increasing up to 70 mm and RF focusing effect without using additional focusing elements.

Figure 8 presents the calculated profiles (Nx=30, Ny=19, Nφ=70) of an average beam current density in the micropulse at the second accelerating gap input (a), in the middle between the third and fourth gaps (b), at the accelerator output (c), and at a distance of 1.5 m from the accelerator output (d). Beam transverse dimensions are shown in millimeters.

Due to injection transverse velocity spread only across the slots, the beam current density profile has an elliptical shape at the second accelerating gap entrance (see Fig. 8a). During beam accelerating RF focusing leads to progressive elimination of this effect in the middle between the third and fourth gaps (Fig. 8b), and at the accelerator output (Fig. 8c). However, in this case the overfocusing of extreme particles takes place, and the beam profile obtains slightly elliptical shape again at a distance of 1.5 m from the accelerator (Fig. 8d). This effect may be eliminated through additional beam magnetic focusing in beam deflecting device at the target.

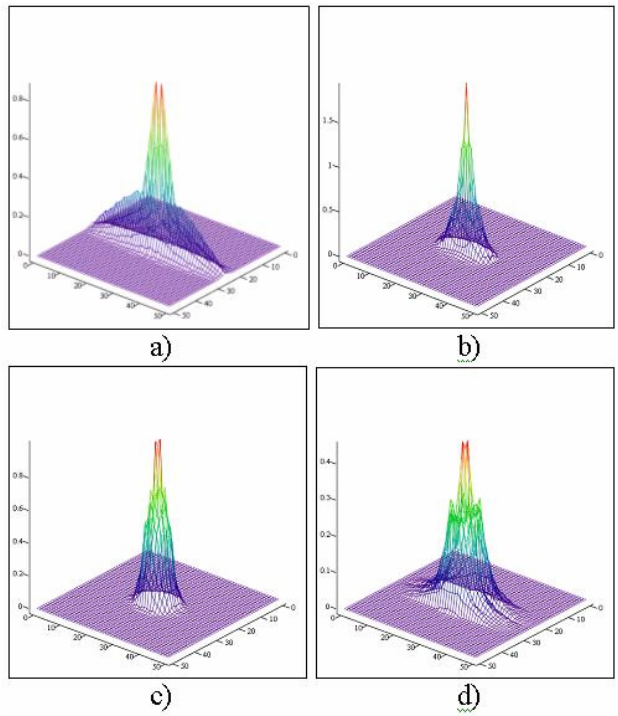

Figure 8: Profiles of an average beam current density at the different stages of accelerating.

CONCLUSION

The results obtained proved the possibility to achieve the required value of the pulse beam current and to transport a powerful electron beam through the accelerating structure without usage of electro- and magnetostatic lenses. It became possible by using the internal beam injection from specially designed cathode-grid assembly with applying a constant biasing voltage and an additional bias RF voltage of operating frequency with appropriate phase shift.

REFERENCES

[1] V. Auslender et al. “High Power Electron Accelerator Prototype”. Proceedings of this conference.

[2] M. Tiunov et al. “5-10 MEV Industrial High Power Electron Accelerator”. Proceedings of EPAC 2002, Paris, France, pp.2813-2815.

[3] B. Fomel, M. Tiunov, V. Yakovlev. “SAM – an interactive code for evaluation of electron guns”. Preprint Budker INP 96-11, 1996.

[4] M. Tiunov, G.Kuznetsov, M.Batazova. “Simulation of High Current Electron and Ion Beam Dynamics for EBIS”, AIP Conference Proceedings, 2001, vol.572, issue 1, pp.155-164.